Tunable Design for LTE Mobile-Phones

Barrio, Samantha Caporal Del; Bahramzy, Pevand; Svendsen, Simon; Jagielski, Ole; Pedersen, Gert Frølund

Published in:
Vehicular Technology Conference (VTC Fall), 2014 IEEE 80th

DOI (link to publication from Publisher):
10.1109/VTCFall.2014.6966218

Publication date:
2014

Document Version
Accepted author manuscript, peer reviewed version

Tunable Design for LTE Mobile-Phones

Samantha Caporal Del Barrio*, Pevand Bahramzy*†, Simon Svendsen†, Ole Jagielski† and Gert F. Pedersen*
*Section of Antennas, Propagation and Radio Networking (APNet), Department of Electronic Systems,
Faculty of Engineering and Science, Aalborg University, DK-9220, Aalborg, Denmark
{scdb,pb, gfp}@es.aau.dk
†Intel Mobile Communications, 35 Lindholm Brygge, Nørresundby 9400, Denmark
{pevand.bahramzy, simon.svendsen, ole.jagielski}@intel.com

***Abstract*—Antenna volume has become a critical parameter in mobile phone antenna design, as broader bandwidths are required for high connectivity between users. Shrinking the antenna size affects its efficiency, if one does not sacrifice bandwidth. This paper proposes an architecture to address the need for small and wide-band antennas. The study focuses on the low-frequencies (700 MHz - 960 MHz) in order to address a tough scenario for small platforms. A tunable design of the front-end and the antennas of the mobile phone is proposed and investigated. Operation is achieved on all low-bands with an efficiency of -3 dB at 700 MHz.**

***Index Terms*—4G mobile communication, Antenna efficiency, Antenna measurements, Reconfigurable antennas, Mobile antennas, Multifrequency antennas.**

I. Introduction

DURING the last decade the development of wireless communication has been major. The ever growing demand for better connectivity has driven the development of the 4^{th} Generation (4G) of mobile communication standards. In order to achieve high data rates 4G specifies the use of Multiple-Input Multiple-Output (MIMO) technology, where several antennas are operating simultaneously at both ends of the radio link. Additionally, each of these antennas should also support a significantly large number of frequency bands. Nowadays, the Frequency Division Duplexing (FDD) spectrum has being extended to 25 bands ranging from 700 MHz to 2.69 GHz for 4G [1]. The bandwidth required for mobile phone antennas is a challenge, as they simultaneously need to be highly integrated and efficient. However, size, bandwidth and efficiency at a given frequency are a trade-off [2].

On the one hand passive antennas have been investigated in order to address the bandwidth issue. Multi-band antennas can cover up to 9 different bands [3], [4], [5]. Parasitic elements have been used for the same purpose [6]. However both techniques lead to increasing the antenna volume. The board resonances can be exploited to obtain compact antennas and broad frequency responses, [7], [8], [9], [10], [11], at the cost of efficiency as well as antenna decoupling limitations [12], [13]. On the other hand active antennas, e.g. Frequency Reconfigurable Antennas (FRAs), are good candidates to provide a wide bandwidth. An additional active component (often switch or tunable capacitor) changes the equivalent reactance of the resulting antenna to modify its resonance frequency. A tunable reactance can continuously shift the resonance frequency of the antenna across a very wide range frequencies. The FRA can achieve an equivalent large bandwidth exhibiting an instantaneous narrow bandwidth.

This paper is structured in four sections. Section II presents the Q formulations that will be used throughout the paper. Section III describes a front-end architecture addressing the bandwidth challenge and the geometry of the antenna design. IV summarizes the measurement results of the antenna. Conclusions are disclosed in Section V.

II. Antenna Quality factor

The Antenna Quality factor (Q_A) is a measure of the stored energy relative to the accepted power in the radiating structure. FRA have a Q_A that increases considerably as the resonance frequency is tuned further away from its original resonance frequency [14]. Along with this increase in Q_A comes a significant radiation efficiency drop, as reported in [15]. The Q_A can also be expressed as a measure inversely proportional to the bandwidth (BW). Dependent on the Voltage-Standing-Wave Ratio (VSWR), Q_A can be expressed as follows [14]:

$$Q_A(\omega) = \frac{2\sqrt{\beta}}{FBW_V(\omega)}, \sqrt{\beta} = \frac{s-1}{2\sqrt{s}},$$

where FBW_V is the matched VSWR fractional bandwidth and s is a specific value of the VSWR.

In practical antenna design, one can distinguish the unloaded Q_A ($Q_{A,unoad.}$) from the loaded Q_A ($Q_{A,load.}$). The $Q_{A,unload.}$ values are found through simulation of a loss-less structure and describe the relation between reactance and resistance in the element itself. They give a worst case scenario, however these values are useful for directly comparing one antenna to another. The $Q_{A,load.}$ values are found through measurements and include the loss in the structure. Evidently $Q_{A,load.}$ values will always be lower than $Q_{A,unload.}$ values. The difference between unloaded and loaded Q_A gives an insight into the amount of loss in the antenna structure.

Simple Q_A calculations on today's bandwidth requirements highlight the challenge of ESA design. In the low-band of 4G communications, the antenna must cover frequencies ranging from 960 MHz to 699 MHz, which corresponds to a Q_A of 3.25. In the case of a FRA with an instantaneous bandwidth of 10 MHz, the corresponding Q_A is 70 at 704 MHz. With these considerations in mind the authors will also name FRA, high-Q antennas.

III. Tunable antenna and front-end

Typically, a FRA is designed at its highest frequency of operation, meaning a small resonator. The tuning mechanism shifts its resonance towards lower frequencies. The main advantage of using FRA is the possibility of having only *one* element that is *small* and that can operate in all the bands. The size reduction of the element is limited by the increase in Q_A and the allowed loss in the antenna structure. Efficiency is a critical parameter in applications where Electrically Small Antennas (ESAs) are required and the transmitter power is limited. In this section the design of tunable antennas for a tunable front-end is described, and its performances are discussed.

A. Tunable Front-End

With the addition of bands to operate in, the front-end design increases dramatically in complexity. One realizes that in order to build a long term solution that can handle the need for bandwidth, an approach with flexible and independent receiving (RX) and transmitting (TX) chains is necessary [16]. Separating the TX from the RX into two autonomous and tunable chains will provide a long term solution to address the expansion of bands added to the spectrum of the next communication generations. The main advantage of this novel architecture is the possibility to remove the duplex filter, which will save cost and space. Eliminating the duplex filters will cancel the need for multiple and redundant RF chains with multiple Power Amplifiers (PA) and Low Noise Amplifiers (LNA). However, the challenge is moved onto the antennas, as two separated and highly isolated antennas are needed. Enough isolation needs to be provided by the antennas – typically 25 dB – to avoid spoiling the signal at the RX. This front-end architecture has been described in more details in [17] and a schematic is added in Fig. 1. The above-described architecture is the frame-work for the proposed antenna design. The design is shown for band 12 in order to address the toughest operating frequencies. The design has two antennas, operating in TX and RX frequencies with 30 MHz duplex distance, as specified in [1] for band 12.

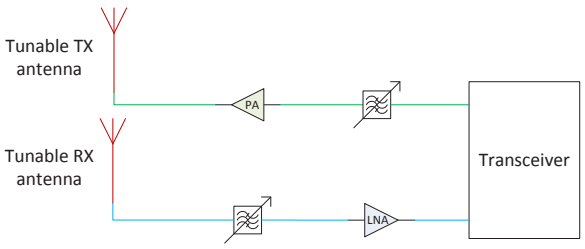

Fig. 1. Tunable front-end architecture [17].

B. Geometry

The geometry of the proposed antennas is depicted in Fig. 2. The Ground Plane (GP) is chosen to be a candy-bar type in order to create a tough scenario at the chosen frequency, and its dimensions are 100×40 mm^2, which represents about

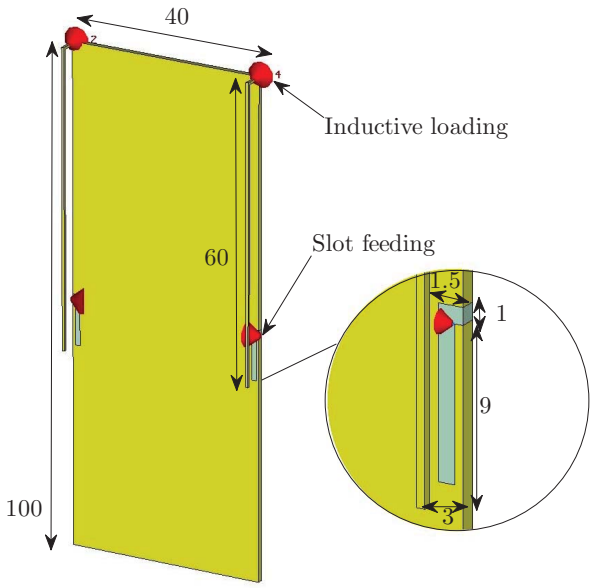

Fig. 2. Small antenna design for handset. Dimensions are given in mm.

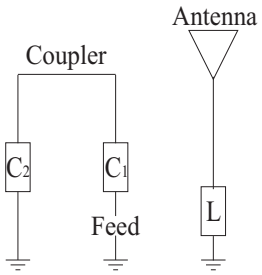

Fig. 3. Antenna diagram.

	TX	RX
L [nH]	34.4	30.0
C_1 [pF]	1.0	1.0
C_2 [pF]	10.0	9.0

TABLE I
Tuning and matching values.

$\lambda/4$ at 700 MHz. The largest dimension of the GP is slightly smaller than $\lambda/4$ at 700 MHz.

The antenna type – for both TX and RX – is a slot-fed monopole placed 3 mm above the GP. The monopole is an inductively loaded wire, exhibiting a length of 60 mm. The feeding happens through coupling with a small slot, cut into the GP. This slot is capacitively loaded and controls the matching – to the 50 Ω impedance feed line – of the resulting design. The slot is filled with FR-4 and placed under the end of the monopole and has dimensions 10×1.5 mm. The inductive loading of the monopole allows a smaller element and the coupled feeding results in a wider bandwidth. Hereafter the authors distinguish the tuning from the matching components used in the proposed design. The tuning components are the inductors and effectively change the resonance frequency of the monopoles; the matching components are the capacitors at the feed that only affect how well the antennas are matched to the feed lines. Both RX and TX antennas have the same length, thus the inductors and matching components have different values in each antenna in order to provide resonances that are 30 MHz apart. In this section the design is shown with fixed lumped components, in order to characterize the performances of small and isolated antennas at 700 MHz on

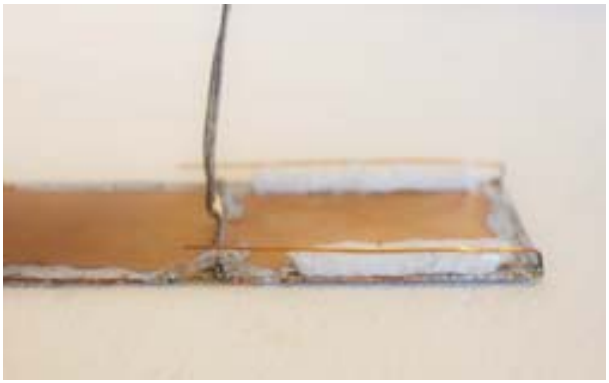

Fig. 4. Mock-up of the small antenna design for handset.

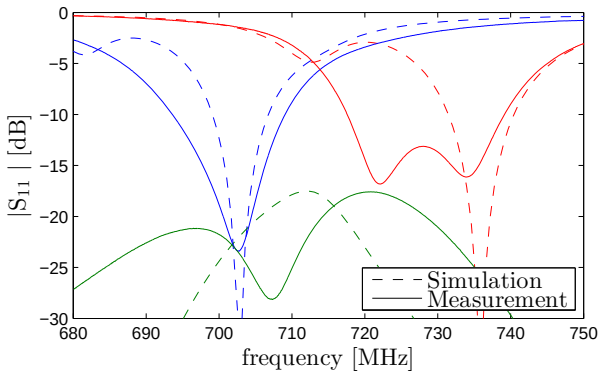

Fig. 5. Simulated and measured frequency responses of the slot-fed monopole in band 12.

a small platform. The component needed for a resonance in band 12 are summarized in Table I and the schematic is represented in Fig. 3. Simulations were run with the Finite Element Method (FEM) solver in CST [18].

IV. Measurements

A mock-up of the above-described design was built for band 12, and it is shown in Fig. 4. Measurements of the two isolated resonances at 700 MHz and 730 MHz are plotted in Fig. 5. The isolation between the TX and RX antennas reaches -20 dB, for bandwidths of 25 MHz and 30 MHz for TX and RX respectively. However with bandwidth of about 10 MHz it is reasonable to expect an isolation below -25 dB. For the proposed architecture, bandwidths of 10 MHz are sufficient in band 12 [19], as the antenna only needs to cover a channel, as opposed to a full band. The differences between the simulations and the measurements lie in a high precision required for the dimensions and placement of the slot and the components. The mock-up was measured in anechoic chamber to evaluate its efficiency with 3D radiation pattern integration technique, and the total efficiency (η_T) is summarized in Table II. The measured η_T of the mock-up with FR-4, tuning and matching components is -5.0 dB for each antenna. Same efficiencies – within the chamber accuracy – are measured for TX and RX antennas. The power lost in the lumped elements can be evaluated in the simulations. The power lost in L (L_L), in C_1 (L_{C_1}) and in C_2 (L_{C_2}) are normalized to 1 W input power and shown in Table II for the TX antenna. From the simulations it can be evaluated that the components are responsible for 4.5 dB of loss in total. The Q values of the components (Q_c) used in the mock-up are also summarized in Table II. It is concluded that most of the loss comes from the matching capacitor C_2, which is placed across the matching slot. Indeed it is placed in a very high current location, even-though it is also placed at the feed. Additionally, because of the high capacitance value needed to match the antenna, its Q_c is very poor. The resulting $Q_{A,load.}$ of the antenna is also summarized in Table II.

As an attempt to reduce the loss in the mock-up, the fixed inductors are replaced by air-inductors made out of the same copper piece as the monopole. The new mock-up is shown in Fig. 6. The inductor consists of only 3 turns as the height of the monopole should remain low. The maximum allowed height

TABLE II
Loss decomposition of the TX slot-fed monopole

η_T [dB] / $Q_{A,load.}$	-5.0 / 55
L_L [dB] / Q_c	1.8 / 88
L_{C_1} [dB] / Q_c	0.1 / 725
L_{C_2} [dB] / Q_c	2.7 / 57

is 3 mm, if one wants to keep the height of the monopole identical to the mock-up containing the fixed inductors and not alter the coupling to the matching slot. For this reason the monopole needs to be extended to both sides of the PCB, as shown in Fig. 7. In order to minimize the antenna isolation the inductors are placed orthogonally. As a result, the η_T has improved almost 2 dB, as summarized in Table III, together with the measured $Q_{A,load.}$ value. This result was expected from the loss decomposition summarized in Table II. However the isolation has worsen to 18 dB. The reason of the drop in isolation between the antennas is twofold: the fields generated by the air-inductors are not as confined as in the case of chip inductors and couple more to each other; and the antennas are more efficient (typically isolation improves with losses, when the antennas are made more efficient more power is radiated, and is likely to couple into the other antenna). The measured S parameters of the mock-up with the air-inductors are shown in Fig. 8.

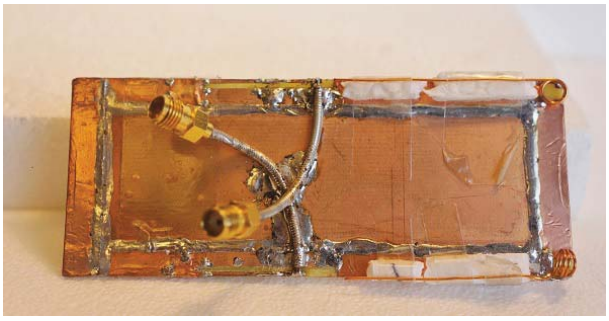

Fig. 6. Improved mock-up with air-inductor (top view).

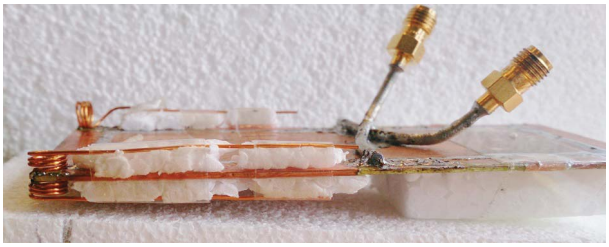

Fig. 7. Improved mock-up with air-inductor (side view).

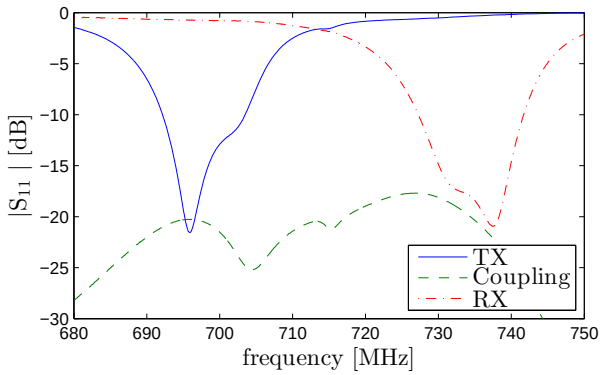

Fig. 8. Measured S parameters of the slot-fed monopole with air-inductors.

V. Conclusion

Efficiently operating at 700 MHz on a small platform is a very challenging task for antenna designers. This paper presents a novel antenna concept, that is designed for a front-end architecture that splits the Tx and the Rx chains. This architecture allows to remove the duplex filters and eliminate redundancies, which leads to saving space, cost and battery life. Consequently, Tx and Rx antennas only need to cover a channel and can exhibit a narrow instantaneous bandwidth, given that they are tunable. Additionally, the antennas need to be highly isolated to provide part of the filtering between the Tx and the Rx chains. The proposed design provides 20 dB of isolation between the antennas at 700 MHz and 730 MHz respectively. It also exhibits -3 dB efficiency at 700 MHz, which is an acceptable value for nowadays market. The antenna measurements show that even using pure copper antennas loaded with air-inductors, a small antenna design at low-frequency is still lossy. This phenomenon is intrinsic to ESAs, when matching and tuning components are needed, as they cause the loss to increase. In the proposed design, size reduction required capacitive matching, which lead to high currents in the matching slot (including components and FR-4), thus relatively high losses. The described antenna design is promising to address the bandwidth challenge on small platforms.

Acknowledgment

The work is supported by the Smart Antenna Front End (SAFE) Project within the Danish National Advanced Technology Foundation, High Technology Platform.

TABLE III
Total efficiency and loaded Q_A of the TX slot-fed monopole with air-inductors

η_T [dB]	-3.0
$Q_{A,load.}$	125

References

[1] 3GPP TS 36.101, "LTE; Evolved Universal Terrestrial Radio Access (E-UTRA); User Equipment (UE) radio transmission and reception," 2013.
[2] R. F. Harrington, "Effect of Antenna Size on Gain, Bandwidth, and Efficiency," *Journal of Research of the National Bureau of Standards-D. Radio Propagation*, vol. 64D, no. 1, pp. 1–12, 1960.
[3] K. R. Boyle and P. J. Massey, "Nine-band Antenna System for Mobile Phones," *Electronics Letters*, vol. 42, no. 5, pp. 5–6, 2006.
[4] P. Ciais, R. Staraj, G. Kossiavas, and C. Luxey, "Compact internal multiband antenna for mobile phone and WLAN standards," *Electronics Letters*, vol. 40, no. 15, pp. 3–4, 2004.
[5] Y.-l. Ban, C.-l. Liu, J. L.-w. Li, and R. Li, "Small-SizeWideband Monopole With Distributed Inductive Strip for Seven-Band WWAN/LTE Mobile Phone," *IEEE Antennas and Wireless Propagation Letters*, vol. 12, pp. 7–10, 2013.
[6] A. Cihangir, F. Ferrero, C. Luxey, G. Jacquemod, and P. Brachat, "A Bandwidth-Enhanced Antenna in LDS Technology for LTE700 and GSM850 / 900 Standards," in *European Conference on Antennas and Propagation (EUCAP)*, no. Eucap, pp. 2706–2709, 2013.
[7] B. K. Lau, J. r. B. Andersen, G. Kristensson, and A. F. Molisch, "Impact of Matching Network on Bandwidth of Compact Antenna Arrays," *IEEE Transactions on Antennas and Propagation*, vol. 54, no. 11, pp. 3225–3238, 2006.
[8] J. Ilvonen, P. Vainikainen, R. Valkonen, and C. Icheln, "Inherently non-resonant multi-band mobile terminal antenna," *Electronics Letters*, vol. 49, pp. 11–13, Jan. 2013.
[9] J. Villanen, J. Ollikainen, and P. Vainikainen, "Coupling Element Based Mobile Terminal Antenna Structures," *IEEE Transactions on Antennas and Propagation*, vol. 54, no. 7, pp. 2142–2153, 2006.
[10] A. Andújar, S. Member, J. Anguera, S. Member, and C. Puente, "Ground Plane Boosters as a Compact Antenna Technology for Wireless Handheld Devices," *Antennas and Propagation, IEEE Transactions on*, vol. 59, no. 5, pp. 1668–1677, 2011.
[11] F. Sonnerat, R. Pilard, F. Gianesello, F. L. Pennec, C. Person, and D. Gloria, "Innovative LDS Antenna for 4G Applications," in *European Conference on Antennas and Propagation (EUCAP)*, no. Eucap, pp. 2696–2699, 2013.
[12] H. Li, Y. Tan, B. K. Lau, Z. Ying, and S. He, "Characteristic Mode Based Tradeoff Analysis of Antenna-Chassis Interactions for Multiple Antenna Terminals," *IEEE Transactions on Antennas and Propagation*, vol. 60, pp. 490–502, Feb. 2012.
[13] H. Li, B. K. Lau, Z. Ying, and S. He, "Decoupling of Multiple Antennas in Terminals With Chassis Excitation Using Polarization Diversity , Angle Diversity and Current Control," *IEEE Transactions on Antennas and Propagation*, vol. 60, no. 12, pp. 5947–5957, 2012.
[14] A. D. Yaghjian and S. R. Best, "Impedance , Bandwidth , and Q of Antennas," *IEEE Transactions on Antennas and Propagation*, vol. 53, no. 4, pp. 1298–1324, 2005.
[15] S. Caporal, D. Barrio, M. Pelosi, G. F. Pedersen, and A. Morris, "Challenges for Frequency-Reconfigurable Antennas in Small Terminals," in *IEEE Vehicular Technology Conference (VTC Fall)*, pp. 1–5, 2012.
[16] J. T. Aberle, "Reconfigurable Antennas for Portable Wireless Devices," *IEEE Antennas and Propagation Magazine*, vol. 45, no. 6, pp. 148–154, 2003.
[17] S. Caporal, D. Barrio, A. Tatomirescu, G. F. Pedersen, and A. Morris, "Novel Architecture for LTE Worldphones," *Antennas and Wireless Propagation Letters*, vol. 12, no. 1, pp. 1676–1679, 2013.
[18] Computer Simulation Technology (CST) http://www.cst.com, "CST Microwave Studio," 2012.
[19] 3GPP Technical Report, "Feasibility study for Further Advancements for E-UTRA (LTE-Advanced) - Specification 36.912 - Release 11," 2012.